

Electronic Transport Properties of Carbon NanoBuds

J. A. Fürst,¹ J. Hashemi,² T. Markussen,¹ M. Brandbyge,¹ A. P. Jauho,^{2,1} and R. M. Nieminen²

¹*Department of Micro and Nanotechnology, DTU Nanotech,*

*Technical University of Denmark, DK-2800 Kongens Lyngby, Denmark**

²*Department of Applied Physics, Helsinki University of Technology, P.O.Box 1100, FI-02015 TKK, Finland*

(Dated: January 7, 2019)

Fullerene functionalized carbon nanotubes – NanoBuds – form a novel class of hybrid carbon materials, which possesses many advantageous properties as compared to the pristine components. Here, we report a theoretical study of the electronic transport properties of these compounds. We use both *ab initio* techniques and tight-binding calculations to illustrate these materials' transmission properties, and give physical arguments to interpret the numerical results. Specifically, above the Fermi energy we find a strong reduction of electron transmission due to localized states in certain regions of the structure while below the Fermi energy all considered structures exhibit a high-transmission energy band with a geometry dependent width.

Carbon nanotubes (CNT) are among the main candidates for post-CMOS nanoelectronic devices because of their high carrier mobility as well as their structural stability. The electronic, optical, and transport properties of CNTs depend strongly on their geometry, offering great versatility, but at the same time posing a huge challenge because of difficulties in growing and isolating CNT's of a predetermined type. Defects, impurities and imperfections, as an inevitable but not necessarily an unfavorable feature of a real-world nanotube, have also attracted intense attention [1], because they can modify the electronic properties of nanotubes to some extent, perhaps even in a controllable way.

Sidewall chemical functionalization of CNTs is already a well-established branch of research (reviews are available in Refs.[2, 3], and recent theoretical progress is reported, e.g. in Refs. [4, 5]). A new member to this family was introduced by the discovery of a hybrid carbon nanostructure, the carbon NanoBud (CNB) [6] consisting of an imperfect fullerene covalently bonded to a single-wall carbon nanotube (SWNT). The CNB's open a new way of functionalizing CNTs, in particular, because of the high reactivity of fullerenes [7, 8] suggests the possibility of further fine-tuning this material via chemical modification.

In order to fully assess the future potential of CNBs a thorough theoretical examination of their properties is necessary. As far as we are aware, only some initial studies of CNBs' electronic structure have been reported thus far [9, 10, 11]. In any device application the conductive properties are of crucial importance. In this work, we undertake a detailed study of the electronic transport properties of CNBs, using both *ab initio* and tight-binding calculations. As we shall show below, the transport properties of the CNBs display certain generic features. We also propose some simple concepts to classify these features, thereby offering general guidelines for future modeling of more complicated structures.

System. The experimentally realized CNBs come in a variety of sizes and shapes [6], and a detailed micro-

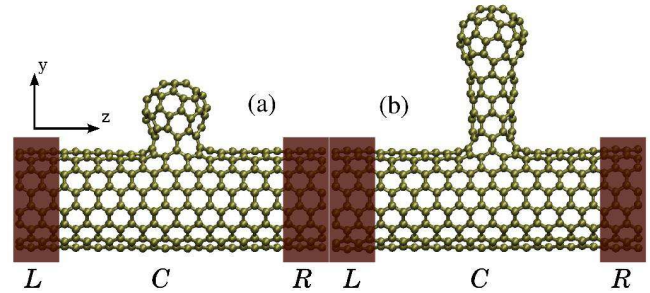


FIG. 1: (Color online) Typical carbon nanobud (CNB) structures studied in this work. The CNB consists of an imperfect C60 attached to an armchair (8,8) single-wall nanotube (SWNT) via a neck region, made of a (6,0) SWNT. The number of unit cells in the neck region can vary; panel (a) shows a zero-unit-cell neck (CNB0), while (b) shows a two-unit-cell neck (CNB2).

scopic knowledge of the exact atomic positions is not yet known. However, in general the CNBs can be categorized in two different groups, depending on how the fullerene is attached to the sidewall of the SWNT [12]. In the first type, a complete fullerene is covalently bonded to a SWNT via sp^3 -hybridization of carbon atoms e.g. [2+2] cycloaddition, while in the second type all carbon atoms are sp^2 -hybridized and the fullerene can be considered as a part of the SWNT. In this work we focus on CNBs in the second group, while the first group will be discussed elsewhere.

Guided by the general features that can be extracted from the available micrographs, and the density-functional calculations on the structural stability reported in Ref. [6], we have chosen to model the CNB structures in the second group as follows (see Fig. 1). The dome of the CNB is an imperfect fullerene, C60, with six atoms removed at the apex. The fullerene is then attached to a (8,8) SWNT via a connecting region ("neck") made of a varying number of unit cells of a (6,0) SWNT. This construction allows a relatively smooth joining of the C60 to the underlying SWNT, even though for

the shortest neck regions the curvature for the connecting bonds is relatively high (see Fig. 1a). We use the notation CNB n , where n is the number of unit cells of the (6,0) SWNT forming the neck, to describe the structures studied in this work. As we will show below, the details of the computed transmission spectra are highly sensitive to the length of the neck, yet they share certain common features.

Computational details. Once the overall structure of the CNB has been decided, we relax the system using the Brenner empirical potential [13] as implemented in the program GULP [14]. We have verified that relaxing the structure in this way leads to insignificant changes in the transport properties as compared to a high quality density functional theory (DFT) relaxation. The size of the supercell is chosen so as to provide 10 Å of vacuum between CNBs in neighboring cells which prevents CNB-CNB interactions. Thus, the supercell size depends on n : $22.5 \text{ \AA} \times (28 + 4.26n) \text{ \AA} \times 34.46 \text{ \AA}$.

The supercell is divided into left (L) and right (R) electrodes containing 64 C-atoms each, and a central region (C) (see Fig. 1).

The transport properties were calculated using the nonequilibrium Green's function method as implemented in the TRANSIESTA code [15], which is built based on an atomic orbital density functional package, SIESTA [16]. The GGA PBE functional [17] was used to describe exchange-correlation, and a mesh cut-off value of 100 Ry defining the real space grid was chosen. A single- ζ basis set was used to reduce the computational cost. To benchmark our settings we relaxed the CNB0 structure and repeated the transmission calculation using a double- ζ polarized basis set with all other parameters unchanged. We found a very good agreement between the results of two different settings, thereby validating the computationally cheaper method.

We have also performed tight-binding (TB) based calculations for the above structures, as well as for larger structures in order to extract the main trends in the transmission properties. The electronic Hamiltonian is described with a nearest-neighbor, orthogonal, sp^3 basis set with TB parameters from Charlier *et al.* [18]. Hopping integrals are calculated within the standard Slater-Koster scheme [19]. All the TB calculations are based on relaxed structures as described above.

However, the restriction to nearest neighbor hopping allows for a more efficient recursive Green's function method as described in Ref. [20], making the TB calculations very fast. All our results are calculated in the zero-bias regime.

Results. Calculated transmissions for three different CNBs are presented in Fig. 2. An immediate observation is that in all cases the conductance is reduced at the Fermi energy and above it. On the other hand, the transmission spectra show a plateau region below E_F where the transmission is the same as for the pristine SWNT.

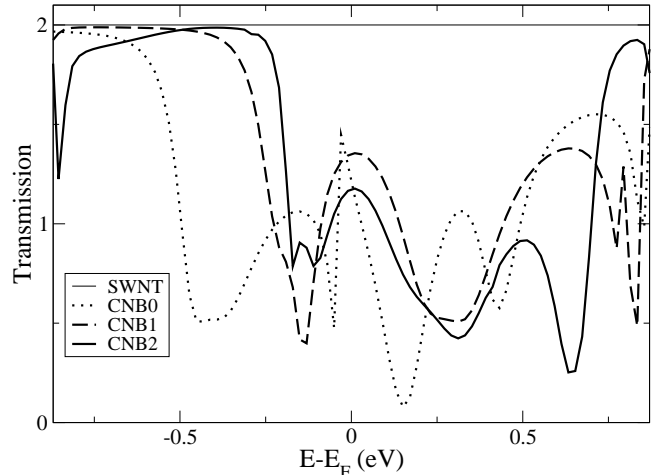


FIG. 2: Transmission as a function of energy for nanobuds CN0, CN1, CN2, and a pristine (8,8) SWNT. For all neck sizes the transmission is strongly reduced except for a plateau region below E_F . With increasing neck length this region shifts upwards in energy and more dips appear at low energies.

The width of this plateau region, however, depends on the length of the neck region (see also Fig. 3 showing CNB3).

Let us next examine the origin for the features in the CNB transmission in more detail. A drop in the transmission can be attributed to two sources. First, vacancies are well-known to reduce the conductance [21, 22, 23, 24], in particular when they are adjacent [22]. The SWNT part of our structures has 6 vacancies and one therefore expects a strongly reduced transmission. Second, localized states in the neck and bud region should cause strong back-scattering. This can be clearly seen in Fig. 3 (top and middle panel) where we show the total projected density-of-states (PDOS) of bud and neck region atoms of CNB3 and the transmission spectrum. (For comparison, for one bulk SWNT unit-cell containing 32 C-atoms the main features of PDOS have values below 1 eV^{-1} and are thus small compared to neck- and bud-PDOS shown in Fig. 3.) All of the dips in transmission have a direct correspondence with a peak in PDOS arising from the states that are localized in the neck and bud regions. Also, in the plateau part of the transmission the bud and neck regions have a very low PDOS and the transmission is essentially the same as for a pristine SWNT. Several features in the transmission spectrum (e.g., at $E - E_F \simeq -0.3, 0.24, \text{ or } 0.8 \text{ eV}$) can be interpreted as Fano (anti-) resonances [25, 26, 27] between the band states in the SWNT and the localized states in the bud and neck region. A similar PDOS-transmission analysis of the region of the SWNT just below the neck reveals that the localized neck and bud states in fact extend some 5 Å into

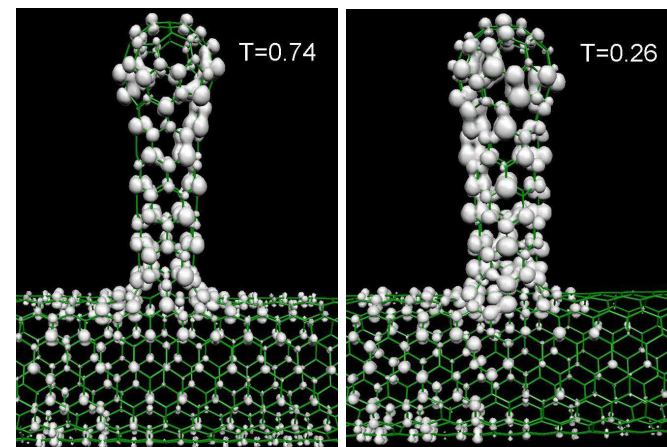
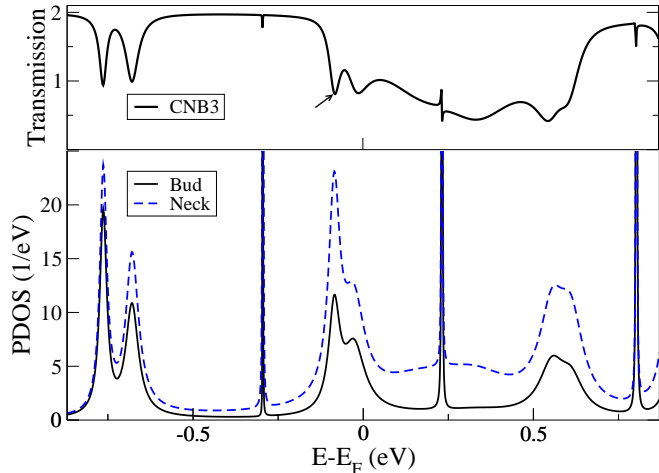


FIG. 3: (Color online) Projected density of states (PDOS) for the bud and neck part of the CNB3 system (middle panel). There is a strong correlation between PDOS and the transmission shown in the top panel. Bottom: The probability of the eigenchannel scattering states at the dip in transmission indicated by an arrow in the top panel. Comparing left ($T = 0.74$) and right panel ($T = 0.26$) shows that stronger reduction of transmission is related to stronger localization of states in the bud and neck.

the SWNT. Thus, it is not obvious how to connect a particular dip in transmission with a particular part of the entire region of localization. Nevertheless, the carbon atoms in this region have a higher reactivity than those located in the underlying SWNT [7, 8]. Therefore, the local electronic structure in the bud/neck regions can be significantly modified, either by chemical adsorption, or by adding functionalizing groups, with a concomitant large change in conductance. If this tuning can be done in a controllable manner it makes CNBs a candidate for a sensitive chemical sensor.

The influence of the neck and bud atoms can be further illustrated by performing an eigenchannel analysis

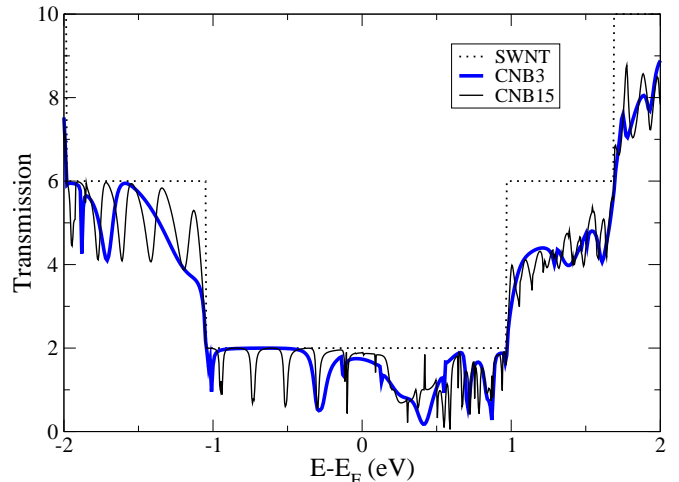


FIG. 4: (Color online) The transmission for SWNT, CNB3 and CNB15 calculated with a tight-binding model. The trends from first principles are well captured for the smaller CNB3 system. Significantly increasing the system size results in a large number of dips which below E_F display some degree of periodicity.

[28] where the scattering states corresponding to elastic eigenchannels at a particular energy are extracted. Fig. 3, bottom panel, shows the scattering states for the two eigenchannels of CNB3 at the dip in transmission indicated by an arrow in Fig. 3, top panel. Comparing the spatial distribution of the scattering states in these two eigenchannels (with transmission probabilities $T = 0.74$ and $T = 0.24$, respectively), one can clearly see that the more the scattering states are localized in the neck and bud regions, the weaker the transmission becomes. Thus, the electron wave function may extend all the way from the tube to the bud, perpendicular to the transport direction. We believe that this feature specific to CNBs has important implications for field emission. Specifically, it is a well-known technological complication that most deposition techniques for SWNT or graphene based field-emitters result in sheets lying flat on the substrate [29]. This is problematic because field emission occurs preferably from tips, protrusions, and high curvature features [30, 31]. CNBs offer a way of avoiding this problem, because there will always be buds aligned with the electric field, and, as our calculations show, the extended states will supply electrons to the bud and neck states. Indeed, a significantly enhanced field emission was observed in the original paper reporting the synthesis of CNBs [6].

Fully *ab initio* calculations for larger CNBs become computationally very demanding. We have studied these structures with the tight-binding (TB) method, which qualitatively reproduces the main trends of the small CNB *ab initio* results. Specifically, the TB-method also

leads to a high transmission band at negative energies (with varying band width), and a reduced transmission at positive energies, though not as dramatic as found with the DFT method. An example is shown in Fig. 3 (top panel, DFT) and Fig. 4 (TB). We attribute this latter discrepancy to a slightly different description of the neck and bud states involved in this energy window in the two methods. Increasing the length of the neck leads to an increase in the number of dips as seen for the CNB15 system shown in Fig. 4. These features can be interpreted as standing electron waves forming in the neck region, in analogy with the analysis presented by Rubio et al. [32] for finite CNTs. Focusing on the energy range $-1.0 - 0.0$ eV in Fig. 4, we identify four dips, with energy separation $\Delta E = 0.21$ eV. Standing waves in a one-dimensional cavity have an energy separation $\Delta E = \hbar v_F \pi / L$, where the Fermi velocity $v_F = 8.5 \times 10^5$ m/s and L is the cavity length. Equating these two expressions for the energy separation yields $L = 8.4$ nm. This is in very good agreement with the CNB15 structure of Fig.4, for which one can associate the length $L_{\text{CNB}} = 8.5$ nm (the combined length for bud and neck is 7.5 nm, and the diameter for the (8,8) SWNT is 1.0 nm). An intriguing feature of all computed transmission spectra is the manifest lack of electron-hole symmetry: the transmission shows much more structures, i.e., rapid oscillations, for positive energies while it remains a relatively smooth function for negative energies. Corresponding rapid oscillations found in the PDOS for the bud/neck region may arise due to closer lying energy levels calculated for a bud/neck molecule. We have, however, not been able to prove this statement quantitatively.

We have also performed calculations on CNBs where the underlying SWNT is semiconducting. Results for (10,0) and (12,0) zig-zag SWNT-based CNBs show, as in the case of metallic tubes, a strongly reduced transmission for positive energies, while there is a plateau of high transmission for negative energies. These results will be discussed elsewhere.

Conclusion. We calculated the transmission spectrum of carbon NanoBuds for various geometries. Two common features emerge: the transmission is significantly reduced at E_F and above it, and high-transmission bands exist for energies below E_F . The electron wave functions may extend to the neck and the bud as well, and are likely to have an effect on the field emission properties of CNBs. The neck region atoms play an important role in the conductance of the system, and suggest that the conductance can be modified by a further manipulation of this region.

Acknowledgment. We gratefully acknowledge numerous discussions with the authors of [6] as well as Martti Puska, Karri Salorittu and Henry Pinto. This work has been supported by the Academy of Finland through its Center of Excellence Program. APJ is grateful to the FiDiPro program of the Academy.

-
- * Electronic address: Joachim.Fuerst@nanotech.dtu.dk
- [1] A. Hashimoto, K. Suenaga, A. Gloter, K. Urita, and S. Iijima, *Nature* **430**, 870 (2004).
 - [2] J.-C. Charlier, X. Blase, and S. Roche, *Rev. Mod. Phys.* **79**, 677 (2007).
 - [3] K. Balasubramanian and M. Burghard, *Small* **1**, 180 (2005).
 - [4] J. M. García-Lastra, K. S. Thygesen, M. Strange, and Ángel Rubio, *Phys. Rev. Lett.* **101**, 236806 (2008).
 - [5] A. López-Bezanilla, F. Triozon, S. Latil, X. Blase, and S. Roche, *Nano Letters* **9**(3), 940 (2009).
 - [6] A. G. Nasibulin, P. V. Pikhitsa, H. Jiang, D. P. Brown, A. V. Krashennnikov, A. S. Anisimov, P. Queipo, A. Moisala, D. Gonzalez, G. Lientschnig, et al., *Nature Nanotech.* **2**, 156 (2007).
 - [7] R. C. Haddon, *Science* **261**, 1545 (1993).
 - [8] F. Diederich and C. Thilgen, *Science* **271**, 317 (1996).
 - [9] T. Meng, C.-Y. Wang, and S.-Y. Wang, *Phys. Rev. B* **77**, 033415 (2008).
 - [10] X. Wu and X. C. Zeng, *ACS Nano* **2**, 1459 (2008).
 - [11] X. Zhu and H. Su, *Phys. Rev. B* **79**, 165401 (2009).
 - [12] A. G. Nasibulin, A. S. Anisimov, P. V. Pikhitsa, H. Jiang, D. P. Brown, M. Choi, and E. I. Kauppinen, *Chem. Phys. Lett.* **446**, 109 (2007).
 - [13] D. W. Brenner, *Phys. Rev. B* **42**, 9458 (1990).
 - [14] J. D. Gale, *JCS Faraday Trans.* **93**, 629 (1997).
 - [15] M. Brandbyge, J.-L. Mozos, P. Ordejón, J. Taylor, and K. Stokbro, *Phys. Rev. B* **65**, 165401 (2002).
 - [16] J. M. Soler, E. Artacho, J. D. Gale, A. García, J. Junquera, P. Ordejón, and D. Sánchez-Portal, *J. Phys.: Condens. Matter* **14**, 2745 (2002).
 - [17] J. P. Perdew, K. Burke, and M. Ernzerhof, *Phys. Rev. Lett.* **77**, 3865 (1996).
 - [18] J. C. Charlier, P. Lambin, and T. W. Ebbesen, *Phys. Rev. B* **54**, R8377 (1996).
 - [19] J. C. Slater and G. F. Koster, *Phys. Rev.* **94**, 1498 (1954).
 - [20] T. Markussen, R. Rurali, M. Brandbyge, and A.-P. Jauho, *Phys. Rev. B* **74**, 245313 (2006).
 - [21] L. Chico, L. X. Benedict, S. G. Louie, and M. L. Cohen, *Phys. Rev. B* **54**, 2600 (1996).
 - [22] H. J. Choi, J. Ihm, S. G. Louie, and M. L. Cohen, *Phys. Rev. Lett.* **84**, 2917 (2000).
 - [23] A. Hansson, M. Paulsson, and S. Stafström, *Phys. Rev. B* **62**, 7639 (2000).
 - [24] M. Igami, T. Nakanishi, and T. Ando, *J. Phys. Soc. Jpn* **68**, 716 (1999).
 - [25] J. A. Furst, M. Brandbyge, A. P. Jauho, and K. Stokbro, *Phys. Rev. B* **78**, 195405 (2008).
 - [26] U. Fano, *Phys. Rev.* **1**, 1866 (1961).
 - [27] J. U. Nockel and A. D. Stone, *Phys. Rev. B* **50**, 17415 (1994).
 - [28] M. Paulsson and M. Brandbyge, *Phys. Rev. B* **76**, 115117 (2007).
 - [29] G. Eda, H. Emrah Unalan, N. Rupeshinghe, G. A. J. Amaratunga, and M. Chhowalla, *App. Phys. Lett.* **93**, 233502 (2008).
 - [30] S. Han and J. Ihm, *Phys. Rev. B* **61**, 9986 (2000).
 - [31] S. Han and J. Ihm, *Phys. Rev. B* **66**, 241402 (2002).
 - [32] A. Rubio, D. Sánchez-Protal, E. Artacho, P. Ordejón, and J. M. Soler, *Phys. Rev. Lett.* **82**, 3520 (1998).